Supporting Information: Nanomechanical and Nanoelectrical Analysis of the Proton Exchange Membrane Water Electrolyzer Anode – Impact of Reinforcement Fibers and Porous Transport Layer

Julian Borowec, Lukas Rein, Nelli Gorin, Shibabrata Basak, Ladislaus Dobrenizki, Günter Schmid, Eva Jodat, André Karl, Rüdiger-A. Eichel, Florian Hausen**

J. Borowec, L. Rein, N. Gorin, Dr. S. Basak, Dr. E. Jodat, Dr. A. Karl, Prof. R.-A. Eichel, Prof. F. Hausen
Institute of Energy Technologies - Fundamental Electrochemistry (IET-1)
Forschungszentrum Jülich GmbH
52425 Jülich, Germany
E-mail: j.borowec@fz-juelich.de, f.hausen@fz-juelich.de

J. Borowec, L. Rein, Prof. R.-A. Eichel, Prof. F. Hausen
Institute of Physical Chemistry
RWTH Aachen University
52074 Aachen, Germany

L. Dobrenizki, Dr. G. Schmid
SE TI SES PRM (Sustainable Energy Solutions - Product - Management)
Siemens Energy Global GmbH & Co. KG
91058 Erlangen, Germany

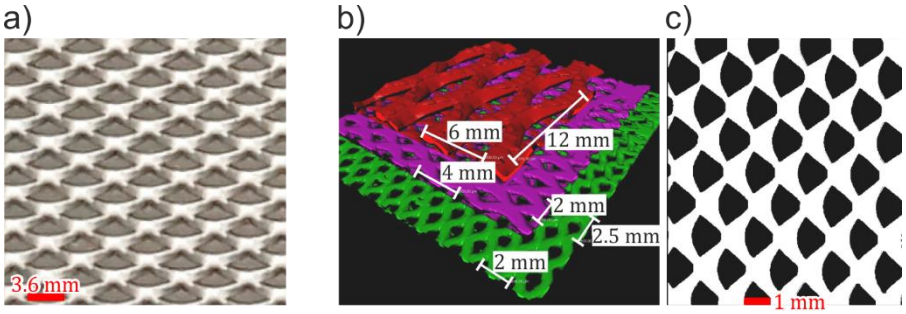

Figure S1: Expanded metal grids are a class of porous transport layers (PTL) in water electrolysis. The principal structure of expanded metal grids comparable to the one utilized within this work is shown with literature examples. a) Top view image of an expanded metal grid. Modified and reproduced with permission.[1] Copyright 2018, Elsevier. b) 3D model of a hierarchically structured expanded metal grid derived from a computed tomography (CT) scan. c) Cross section of a 3D scan shows the expanded metal material (white) and the channels (black). b) and c) are modified and reproduced with permission.[2] Copyright 2023, Elsevier. The X-like PTL interface and triangle-like PTL channel interface features found on the operated anode, shown in Fig. 2b, match with herein shown general expanded metal grid features from literature.

a)

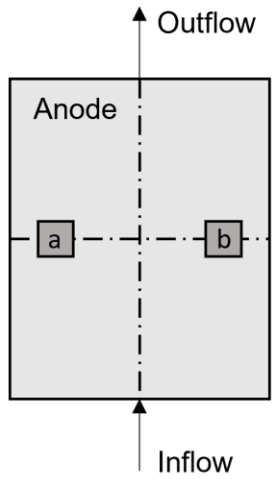

b)

Acquired 5 µm x 5 µm AFM images for each sample a/b

Pristine:

- 3x above reinforcement fiber intersection
- 3x between reinforcement fiber intersection

Operated:

- 3x above reinforcement fiber intersection
- 3x between reinforcement fiber intersection
- 3x PTL mark above reinforcement fiber intersection
- 3x PTL mark between reinforcement fiber intersection

Acquired 360 µm x 360 µm nanoindentation maps for each sample a/b:

- 2x pristine
- 4x operated

Figure S2: a) The scheme of the MEA shows the location of the analyzed samples. The samples were cut from a position between water inflow and outflow. To enhance statistics two symmetrically located samples sample-a and sample-b were cut from the MEA and analyzed. b) The list shows the acquired data on each of the two samples (a and b), which were cut from each MEA, pristine and operated.

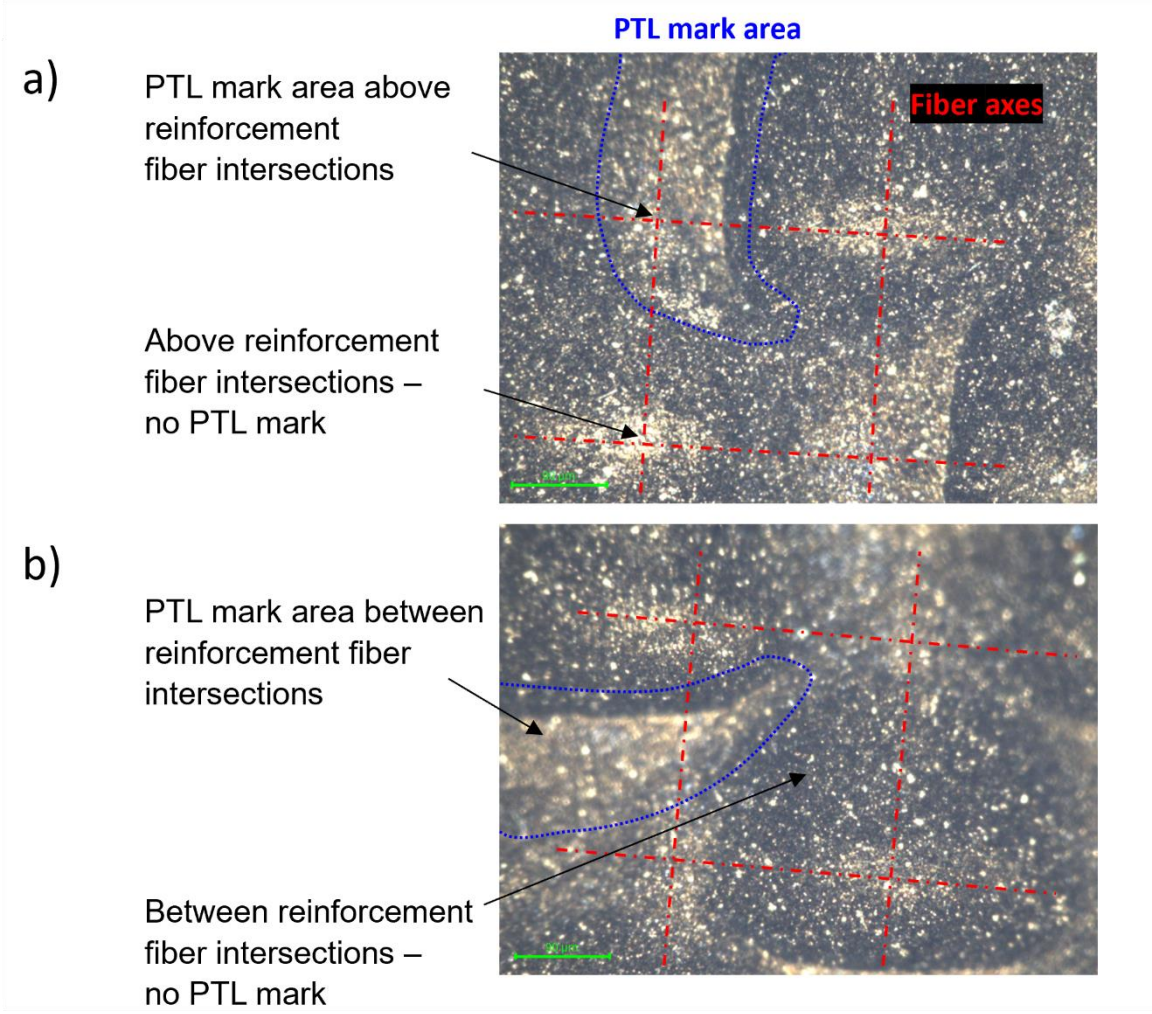

Figure S3: To distinguish influences of reinforcement fibers, the experiments and subsequent analysis were performed with respect to the position of reinforcement fiber intersections. a) Optical microscope image in which a part of the PTL mark area overlaps with an underlying reinforcement fiber intersection, especially around the labelled arrow. b) PTL mark area that is not overlapping with underlying reinforcement fiber intersections.

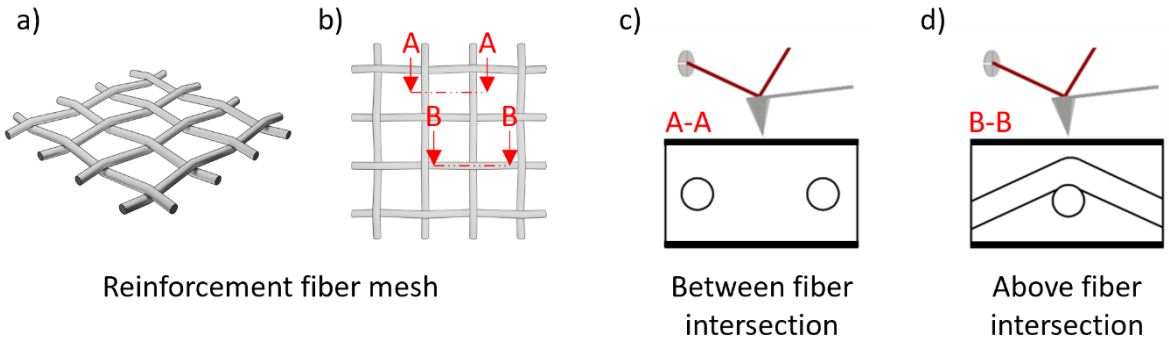

Figure S4: The terms between and above reinforcement fiber intersections, described in Figure S2, are displayed in more detail. a) The scheme highlights the web-woven structure of the reinforcement fiber mesh, located in the membrane bulk. b) The reinforcement fiber's mesh top view indicates the location of cross sections A-A and B-B, that are displayed in the following for a membrane electrode assembly (MEA). c) MEA cross section at a location between fiber intersections with respective probe positioning. d) MEA cross section at a location above reinforcement fiber intersections with respective probe positioning.

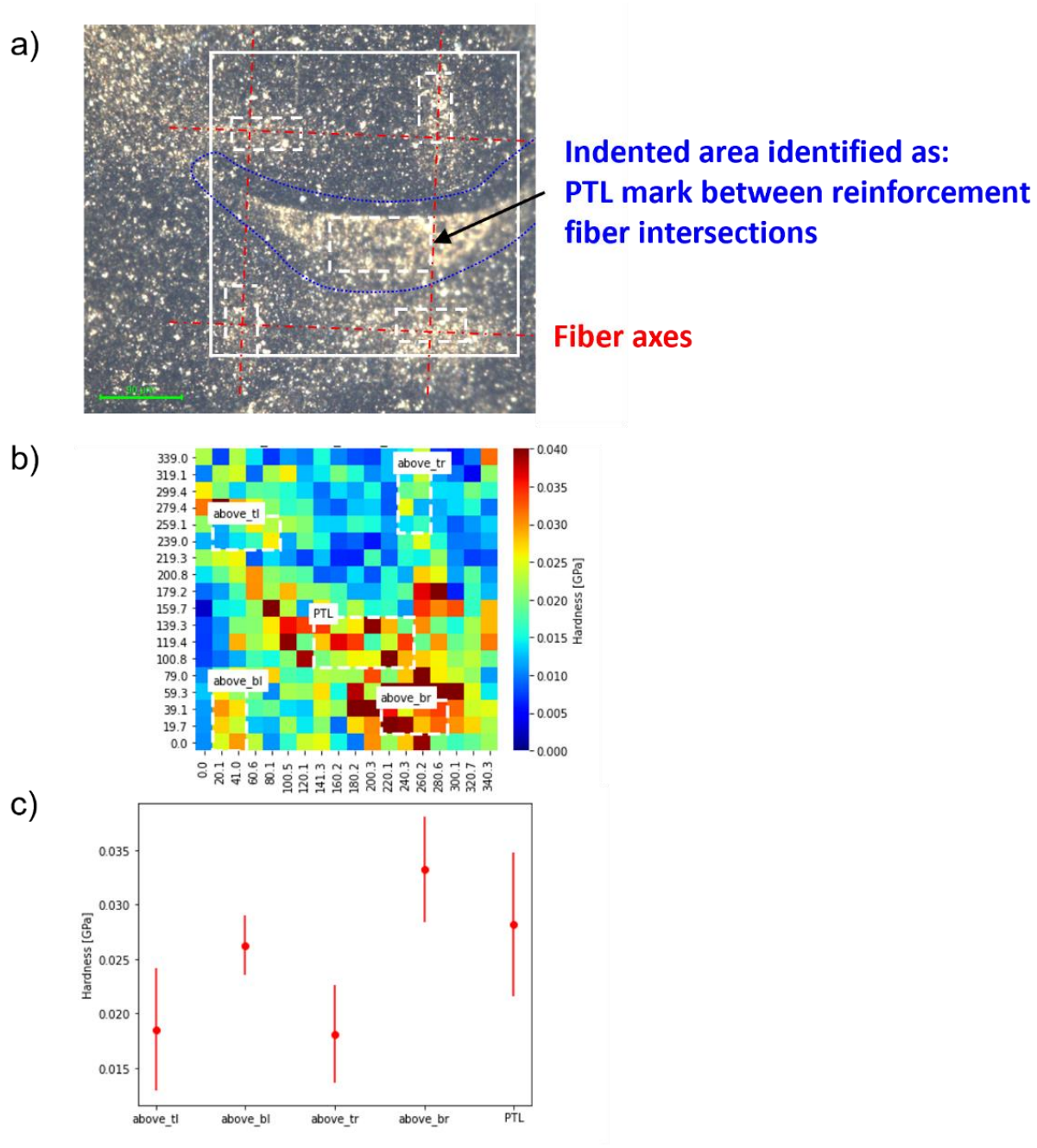

Figure S5: a) An exemplary nanoindenter's optical microscope image of an operated anode is displayed. Depending on the optical microscope image features, the individual indents of the nanoindentation maps were classified into the features of interest: above reinforcement fiber intersection, between reinforcement fiber intersections and additionally regarding the presence or absence of PTL marks. The approximate fiber axes and PTL mark position are indicated. b) The hardness map corresponding to the white boxed area in image a) is displayed. On the x- and y-axis the distance in µm is given with discrete values for the indent positions. The based on the optical microscope image identified features, are marked by the white dashed rectangles. Each hardness value within one rectangle is averaged and given in c). For comparison across the sample the mean hardness values of multiple equivalent features over multiple maps are averaged again. The same approach is valid for the reduced modulus calculation.

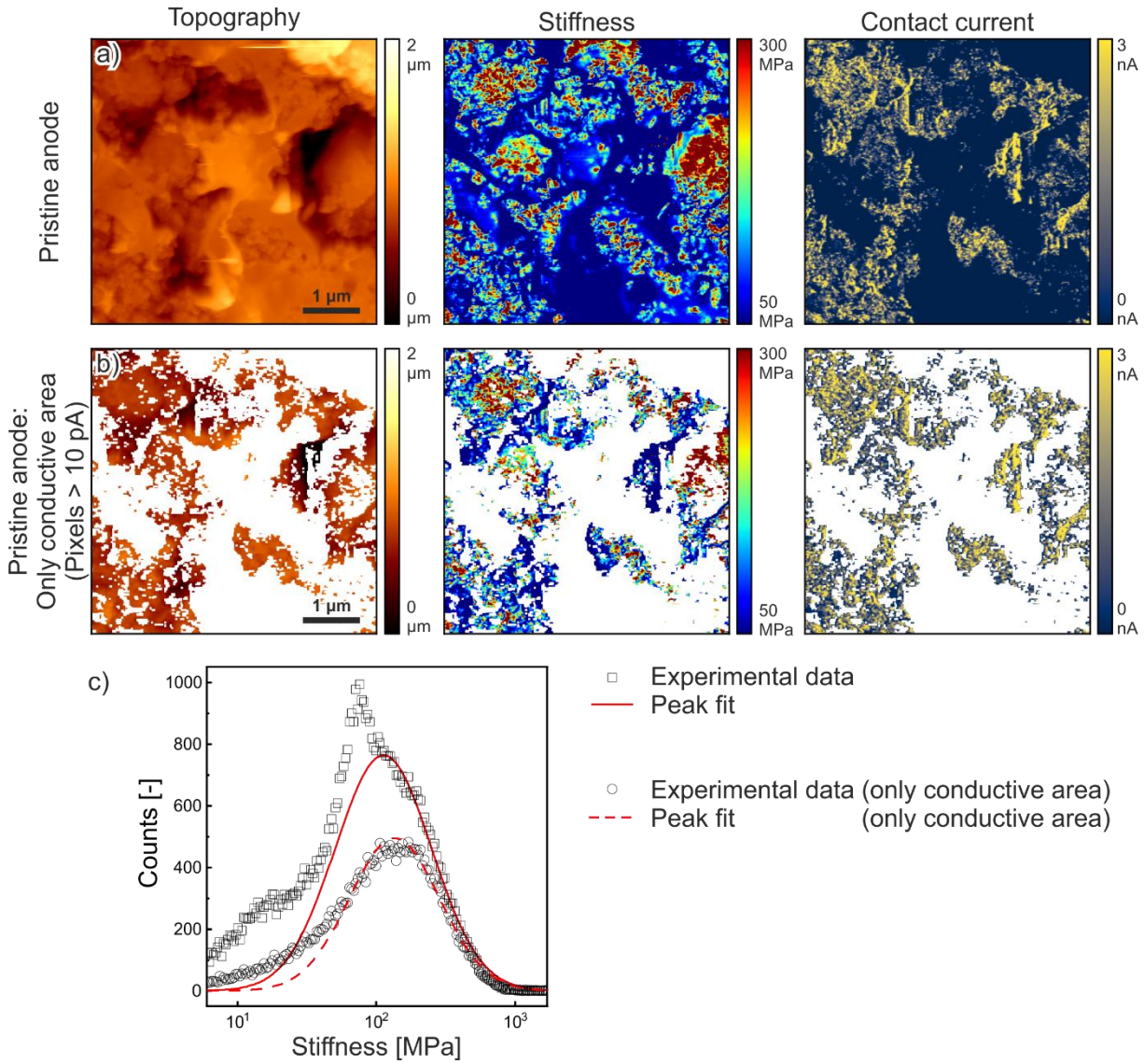

Figure S6: a) Topography, stiffness and contact current maps of a pristine anode are shown. b) To identify the area, which is for sure catalyst area, the same maps are shown with only pixels, that exhibit electrical currents above background noise (>10 pA). c) The stiffness histograms of a) and b) are displayed. While the unfiltered stiffness histogram displays a sharp peak around 90 MPa, it is not visible anymore in the histogram displaying only the conductive area. Therefore, the sharp peak is associated with the electrically non-conductive ionomer. The higher stiffness peak consists mostly of the conductive pixels and is therefore associated with the catalyst.

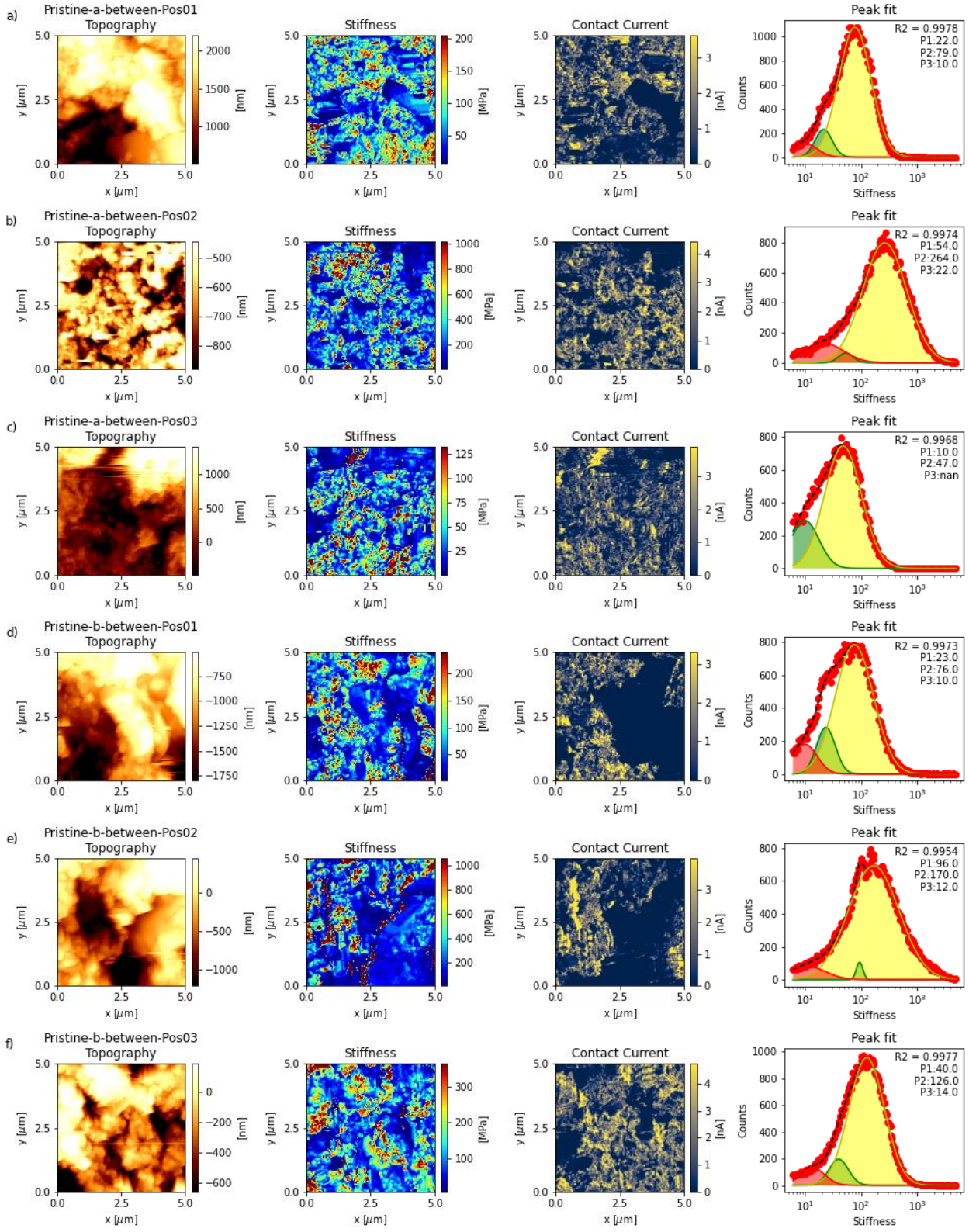

Figure S7: a)-f) Topography, stiffness, contact current maps, and stiffness peak fits of the pristine anode between reinforcement fiber intersections are shown. Yellow peak fits (P2) are associated with the catalyst, as these peaks mostly consist of the electrically conductive area, such as exemplary shown in Figure S6.

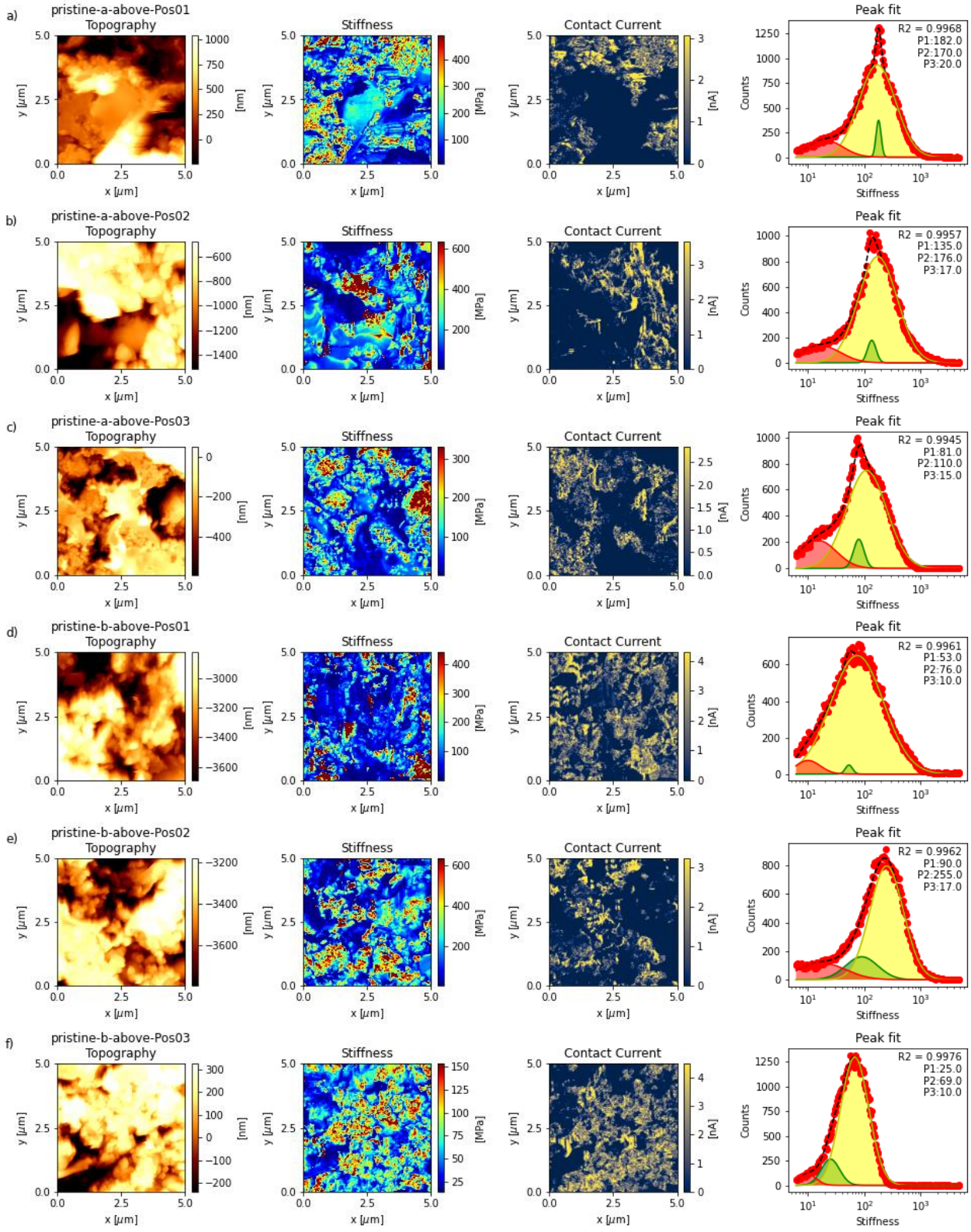

Figure S8: a)-f) Topography, stiffness, contact current maps, and stiffness peak fits of the pristine anode above reinforcement fiber intersections are shown. Yellow peak fits (P2) are associated with the catalyst, as these peaks mostly consist of the electrically conductive area, such as exemplary shown in Figure S6. Prominent sharp green peaks (P1), which are especially observed in a)-c) are associated with ionomer, as these contain pixels, which are electrically non-conductive, such as shown in Figure S6.

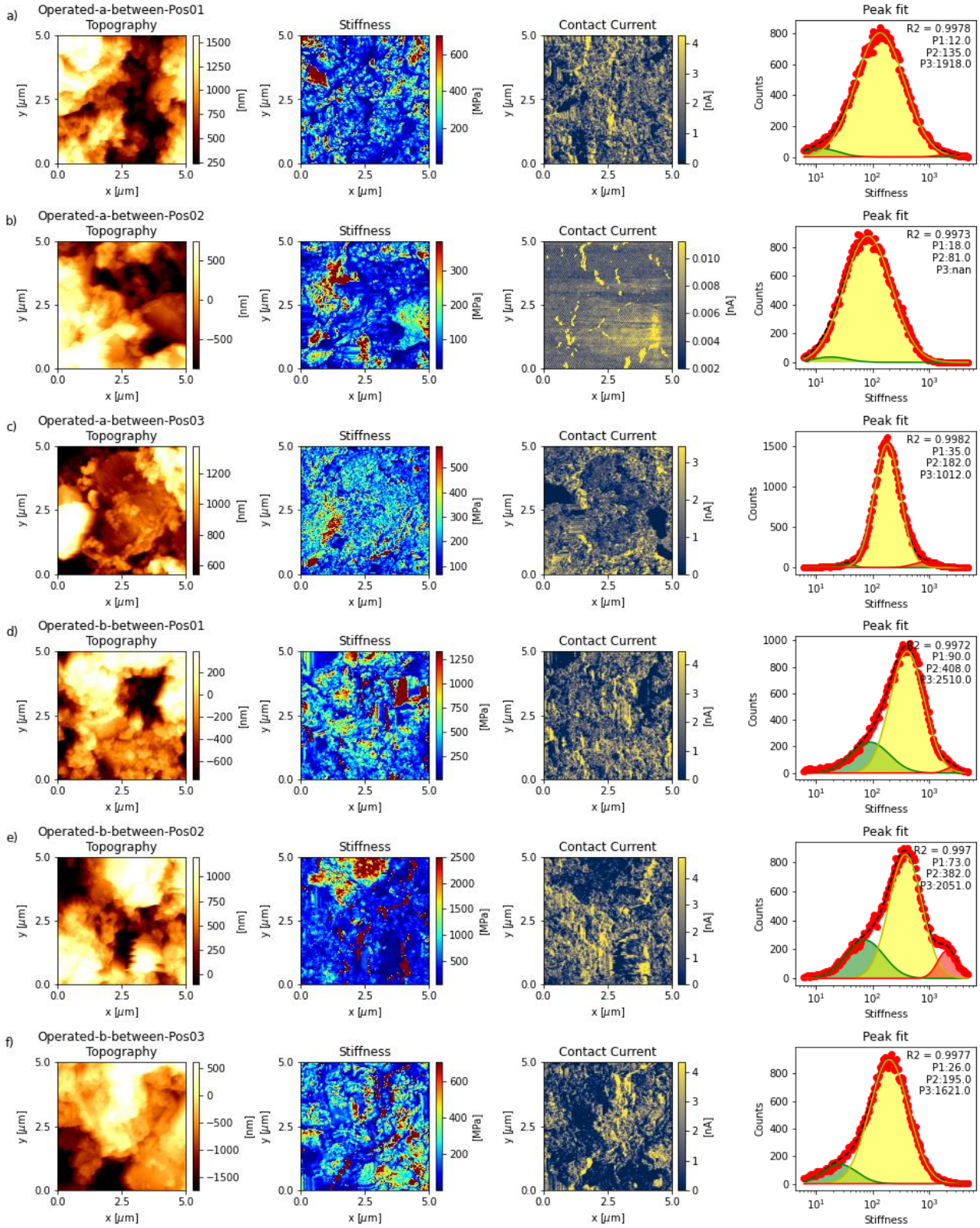

Figure S9: a)-f) Topography, stiffness, contact current maps, and stiffness peak fits of the operated anode between reinforcement fiber intersections at spots without PTL marks are shown. Yellow peak fits (P2) are associated with the catalyst, as these peaks mostly consist of the electrically conductive area, such as exemplary shown in Figure S6. The contact current map in b) shows no signal, which is associated with a missing connection from voltage source to tip. A significantly large high-stiffness peak associated with contaminations (red P3) is observed in e).

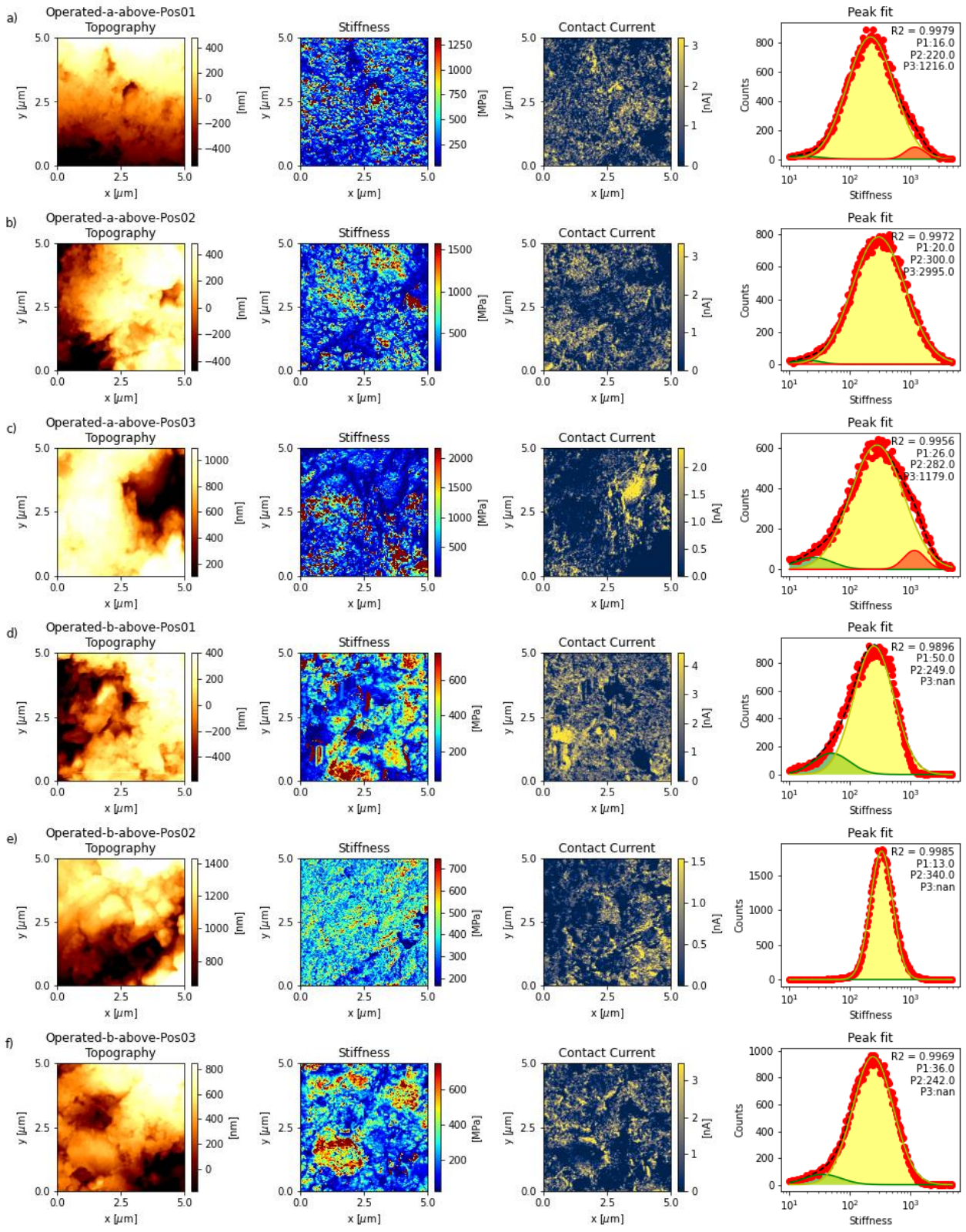

Figure S10: a)-f) Topography, stiffness, contact current maps, and stiffness peak fits of the operated anode above reinforcement fiber intersections without PTL marks are shown. Yellow peak fits (P2) are associated with the catalyst, as these peaks mostly consist of the electrically conductive area, such as exemplary shown in Figure S6. High-stiffness peaks associated with contaminations (red P3) are observed in a), c), and f).

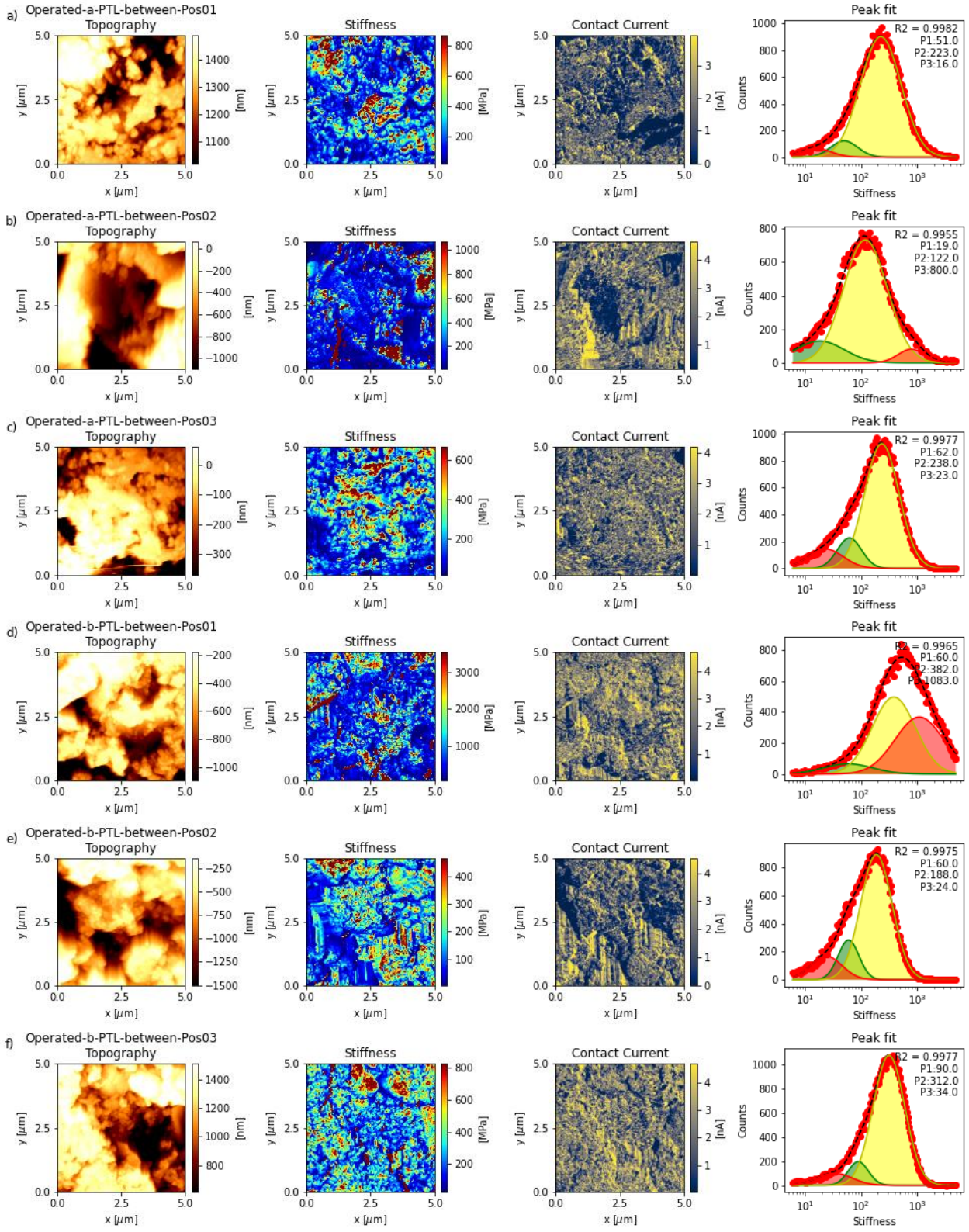

Figure S11: a)-f) Topography, stiffness, contact current maps, and stiffness peak fits of the operated anode at PTL marks between reinforcement fiber intersections are shown. Yellow peak fits (P2) are associated with the catalyst, as these peaks mostly consist of the electrically conductive area, such as exemplary shown in Figure S6. High-stiffness peaks associated with contaminations (red P3) are observed in b) and d).

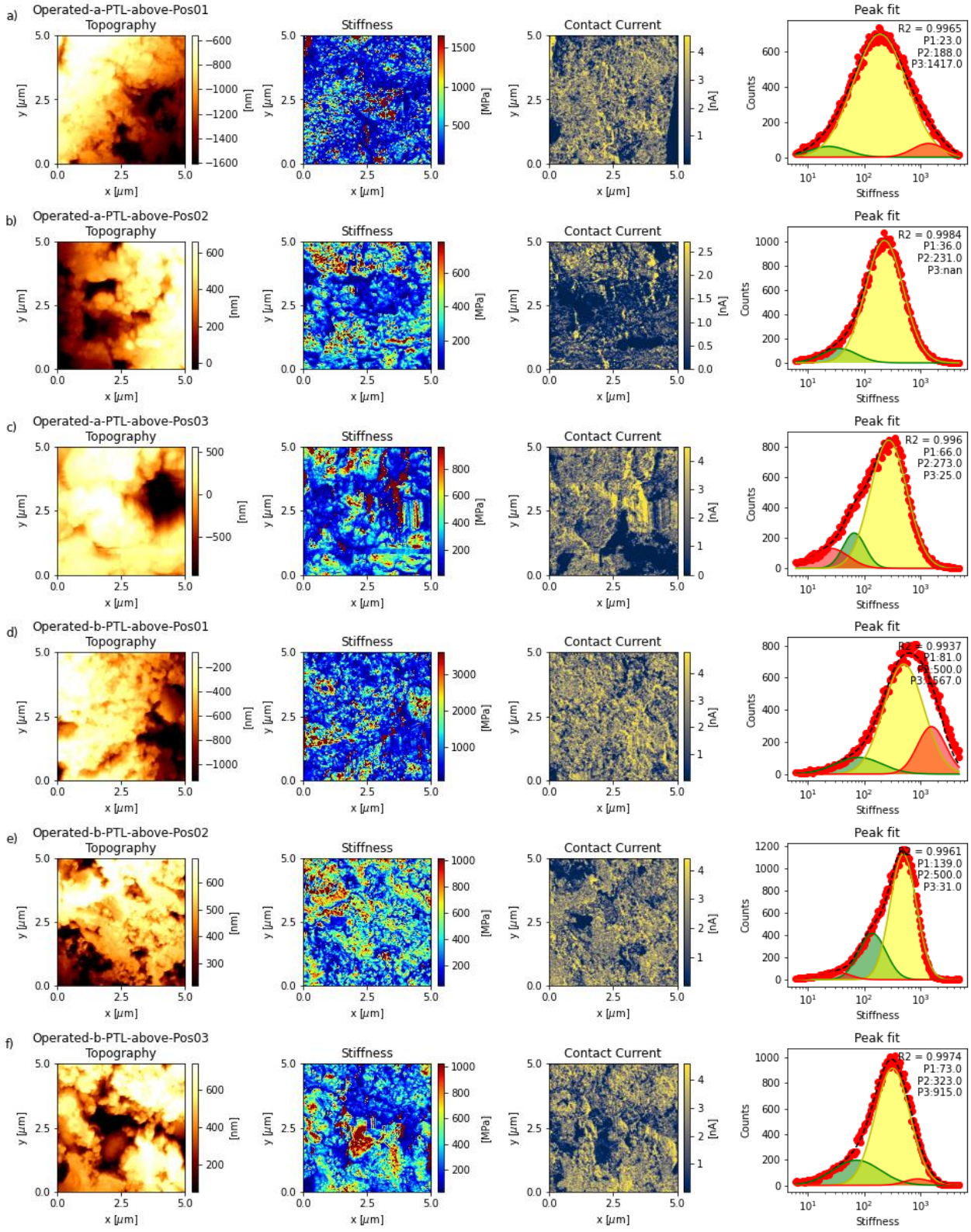

Figure S12: a)-f) Topography, stiffness, contact current maps, and stiffness peak fits of the operated anode at PTL marks above reinforcement fiber intersections are shown. Yellow peak fits (P2) are associated with the catalyst, as these peaks mostly consist of the electrically conductive area, such as exemplary shown in Figure S6. High-stiffness peaks associated with contaminations (red P3) are observed in a), d), and f).

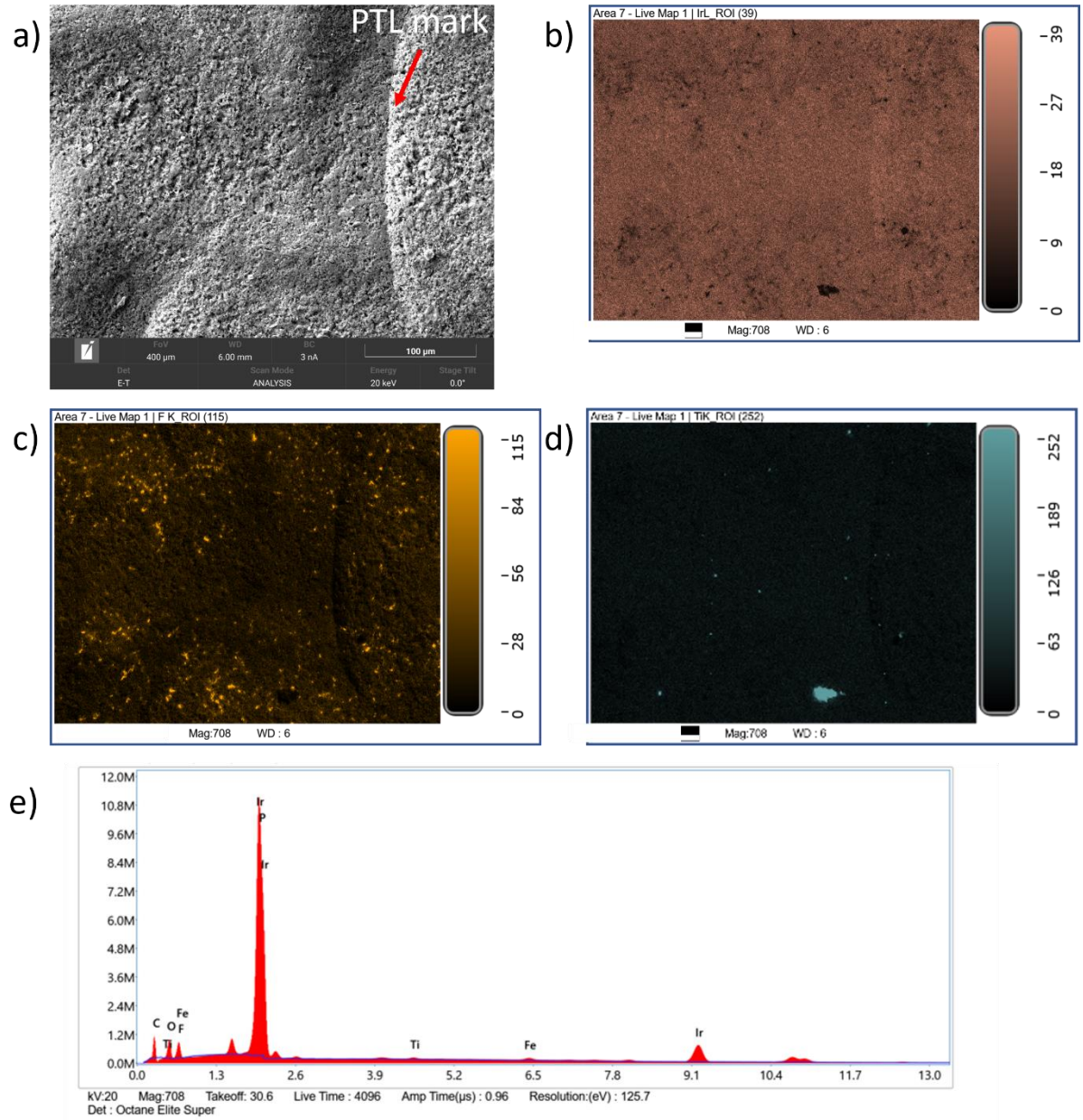

Figure S13: a) A scanning electron microscopy (SEM) image of an operated anode with a PTL mark on the right side is shown. b) The energy dispersive spectroscopy (EDS) map shows that Ir is distributed all over the analyzed area. c) Some spots exhibit less Ir and therefore, a higher F concentration. A few µm sized particles of Ti are found all over the sample, which are associated with the Ti PTL that was in contact with the anode during operation. e) The EDS spectrum indicates that besides Ti, traces of Fe contaminations might be present as contaminant.

References

[1] Lafmejani, Saeed Sadeghi, et al. "Experimental and numerical study of flow in expanded metal plate for water electrolysis applications." *Journal of Power Sources* 397 (2018): 334-342.
[2] Hoppe, Eugen, et al. "An ex-situ investigation of the effect of clamping pressure on the membrane swelling of a polymer electrolyte water electrolyzer using X-Ray tomography." *Journal of Power Sources* 578 (2023): 233242.